Molecular Crystals and Liquid Crystals Science and Technology. Section A. Molecular Crystals and Liquid Crystals

Publication details, including instructions for authors and subscription information:
http://www.tandfonline.com/loi/gmcl19

The Reduction of the Irreversible Capacity of Metal Oxide-Based Negative Electrodes for Li-Ion Batteries

Pier Paolo Prosini [a], Majka Carewska [a], Francesco Cardellini [a] & Stefano Passerini [a]

[a] ENEA, C.R. Casaccia, Via Anguillarese 301, S. Maria di Galeria, Rome, 00060, Italy

Version of record first published: 24 Sep 2006

To cite this article: Pier Paolo Prosini, Majka Carewska, Francesco Cardellini & Stefano Passerini (2000): The Reduction of the Irreversible Capacity of Metal Oxide-Based Negative Electrodes for Li-Ion Batteries, Molecular Crystals and Liquid Crystals Science and Technology. Section A. Molecular Crystals and Liquid Crystals, 340:1, 437-448

To link to this article: http://dx.doi.org/10.1080/10587250008025506

Mol. Cryst. and Liq. Cryst., 2000, Vol. 340, pp. 437-448
Reprints available directly from the publisher
Photocopying permitted by license only

The Reduction of the Irreversible Capacity of Metal Oxide-Based Negative Electrodes for Li-Ion Batteries

PIER PAOLO PROSINI, MAJKA CAREWSKA, FRANCESCO CARDELLINI and STEFANO PASSERINI

ENEA, C.R. Casaccia, Via Anguillarese 301, S. Maria di Galeria, Rome 00060, Italy

Metal oxide-based negative electrodes have received great attention in recent years mainly for their large lithium insertion capacity. Tin-based amorphous oxides have shown to reversibly intercalate about 600 mAh of lithium per gram of oxide. Unlikely, the use of these materials in practical cells is reduced by the irreversible uptake of lithium that takes place during the first insertion/release cycle. In this paper we show that the irreversible capacity of a non-stoichiometric lithium iron oxide (Li-Fe-O) can be substantially reduced through a preliminary chemical reaction with lithium hydride at high temperature (600°C).

Keywords: lithium iron oxide; negative electrode; lithium ion batteries

INTRODUCTION

The introduction of carbonaceous materials (graphite and cokes) as lithium intercalation anodes has allowed the wide commercialization of rechargeable lithium batteries usually called lithium-ion. The wide interest developed on the

investigation of new lithium intercalation negative electrodes has led to the identification of several materials. Cobalt nitrides [1], manganese nitrides [2] and transition metal oxides characterized by a low intercalation potential such as WO_2 and MoO_2 [3], Nb_2O_5 [4], $Li_4Ti_5O_{12}$, $Li_4Mn_5O_{12}$, $Li_{12}Mn_4O_9$ [5], $Li[Li_{1/3}Ti_{5/3}]O_4$ [6], TiO_2 [7], and$CuCoS_3O_8$ [8], have received great attention. They present high reversibility for lithium insertion but their capacity is somewhat limited.

Recently, Idota et al. [9,10], have shown that amorphous tin oxides have very high capacity (0.6 Ah/g) for lithium intercalation. Unlikely, such a performance is also accompanied by a large irreversible capacity in the first cycle. Dahn et al. [11] have shown that the initial irreversible capacity is related with the reaction of lithium and the oxide to form lithium oxide and metallic tin. Further lithium intercalation leads to the mostly reversible formation of a Li-Sn alloy [12,13].

Iron oxides have also been proposed as intercalation negative electrodes because of their availability and low price. Ohzuku et al. have electrochemically reduced Fe_2O_3. They found that two equivalents of lithium were inserted and proposed the formation of FeO and Li_2O [14]. In a following work, Scrosati et al. prepared Li_6FeO_3 by exhaustive electroreduction of Fe_2O_3 and demonstrated its use as alternative anode in lithium batteries [15]. Abraham et al. prepared $Li_xFe_2O_3$ via a room temperature reaction involving the in situ generation of Li-naftalide in tetrahydrofurane [16]. More recently, sodium ferrite Na_2O-$1.5Fe_2O_3$ electrode was tested as alternative negative electrode whit a reversible specific capacity of up to 0.36 Ah/g. The material showed an irreversible behavior on the first cycle where the cycle efficiency was about 51% [17]. Unlikely, iron oxides share with tin oxides large initial irreversible capacities. Only a fraction of the lithium inserted in the first cycle is available in the following release cycle and this leads to a low overall capacity of the battery. The present work is an attempt to ex-situ reduce the irreversible capacity of a lithium iron oxide in order to make feasible the use of iron oxide-based negative electrodes in lithium-ion batteries.

EXPERIMENTAL

Lithium iron oxide (Li-Fe-O) was prepared by reacting 3.714 grams of Li_2CO_3 (Carlo Erba, Reagent Grade) with 11.577 grams of Fe_2O_3 (Aldrich, Reagent Grade) at 850°C for 10 hours. Prior thermal treatment the powders were dried at 120°C (18 hrs) then mixed with 50 cc of acetone and grounded in an orbital mill for 30 minutes. The resulting material is a single phase Li-Fe-O compound. XRD measurements (see later Figure 3, lower curve) have indicated that the material does not belong to any of the known phase of Li-Fe-O. Further studies are presently in progress to fully characterize its crystalline form.

Ex-situ reduced Li-Fe-O materials (later called rLi-Fe-O) were prepared by reaction of $LiFeO_2$ with LiH in argon atmosphere. The starting materials were weighed to obtain a pre-defined ratio, mixed and loaded in argon filled dry box (H_2O and O_2 <1 ppm). The mixture of materials was heated at 600°C for 15' in an alumina crucible under argon flux. After cooling a gray colored product was recovered. Three different materials were prepared by using 1.5, 2 and 3 equivalents of LiH per mole of iron.

Composite cathode tapes were made by roll milling a mixture of 60% active material, 30% binder (Teflon, DuPont) and 10% carbon (SuperP, MMM Carbon). Electrodes were punched in form of discs typically with a diameter of 8 mm. A typical electrode weighed 4.2 mg corresponding to an active material mass loading of 5 mg/cm^2. The electrodes were assembled in two-electrodes electrochemical sealed cells formed by polypropylene T-type pipe connectors with three cylindrical stainless steel (SS316) current collectors. Lithium foils were used as both counter/reference electrode while glass fiber discs were used as separators. The cell was filled with propylene carbonate/$LiClO_4$ (1M) electrolytic solution. Cells were tested with constant current charge/discharge cycles (typically 60 μA/cm^2, 12-17 mA/g) between fixed voltage limits (3-0.5 Volt vs. Li). The cycling tests were carried out automatically by means of a battery cycler (Maccor 2000).

Composite cathode preparation, cell assembly, test and storage were performed in a dry room (R.H. < 0.2%).

XRD patterns of pristine as well as electrochemically lithiated samples were obtained by means of an Italstructures diffractometer using a focused Co kα radiation and equipped with a PSD (INEL) curved detector.

RESULT & DISCUSSION

Figure 1 illustrates the quasi-equilibrium voltage of a Li-Fe-O composite electrode as a function of the inserted lithium content. The electrochemical

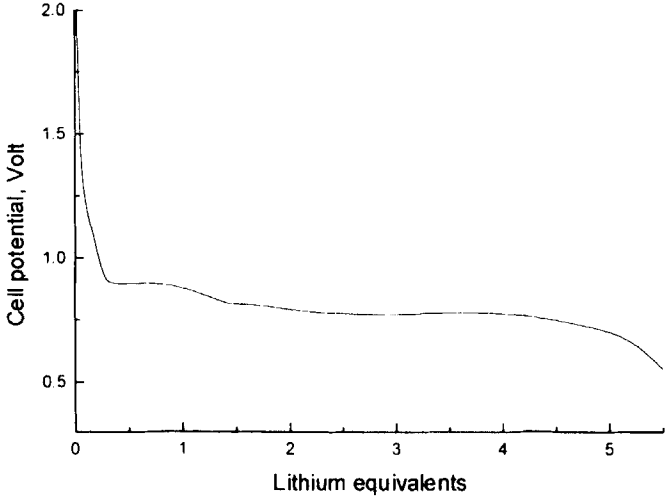

FIGURE 1 Quasi-thermodynamic voltage vs. composition behavior of a Li-Fe-O electrode.

lithium insertion was driven at a very low current density (60 μA/cm^2, 17 mA/g) in order to fully lithiate the electrode and to avoid large polarization and

ohmic overvoltages. After an initial steep drop the voltage curve shows a plateau at 0.9 V (vs. Li) that extends for about 0.5 equivalents of lithium. Upon further lithium insertion the voltage slowly declines to reach a second, mostly flat region located around 0.8 V (vs. Li). This region extends for about three equivalents of lithium. It is composed of several parts identified by relatively small voltage fluctuations that could be associated to different processes. Finally a third region, in which the voltage gradually declines down to 0.5 V (vs. Li), is seen in the figure. This final region was previously attributed to electrolyte decomposition[16,17].

The lithium insertion process is not completely reversible as indicated by the modification shown in the differential capacity plot reported in Figure 2.

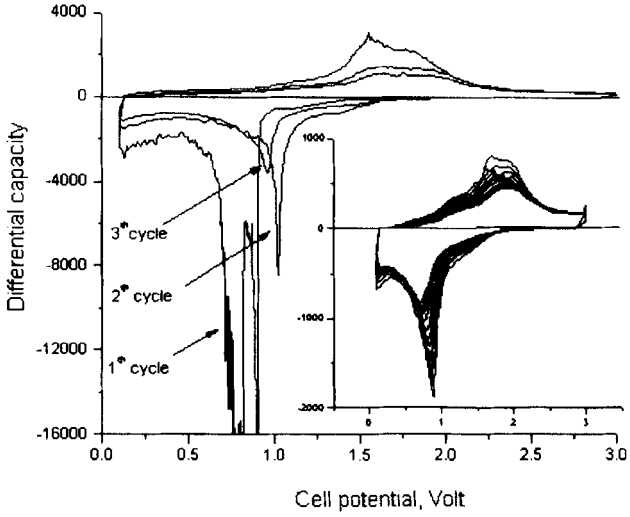

FIGURE 2 Differential capacity vs. electrode voltage behavior of a Li-Fe-O electrode. The figure refers to the first three cycles while the inset illustrates the behavior in following cycles.

The experiment was performed by cyclically driving the lithium insertion and

release process in galvanostatic conditions. During the first cycle the lithium insertion proceeds through different steps as indicated by the presence of two cathodic peaks. The features can be easily associated with the voltage plateaus seen in Figure 1. In the second cycle the peak moves toward higher voltages at about 1.02 V (vs. Li). From the third cycle, the cathodic peak shifts back to lower voltages to finally stabilize (see inset) at about 0.7 V (vs. Li). In addition, the peak broadens on cycling thus indicating a widening of the voltage change in the insertion plateau. These effects can be related to a severe modification of the crystalline structure of the material during the first intercalation cycle and, at a lower extent, the following cycles. To verify this hypothesis, a structural characterization of the material was performed. Figure 3 depicts the diffraction patterns of a pristine (lower curve) and a fully lithiated (upper curve) Li-Fe-O electrode pellets.

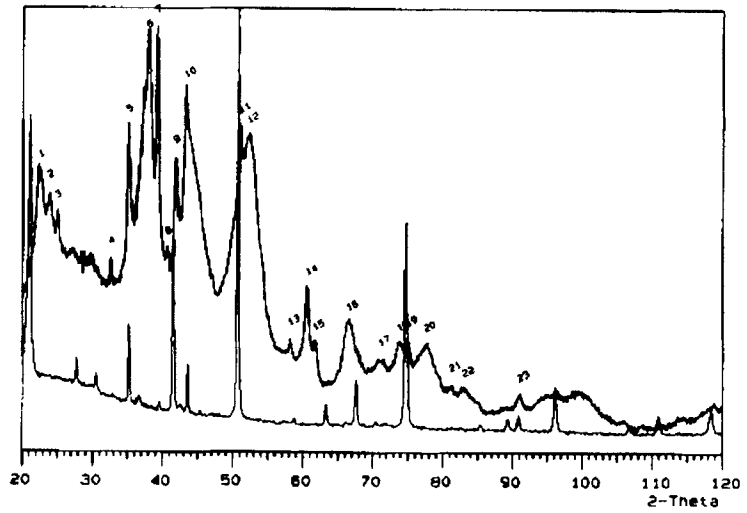

FIGURE 3 XRD patterns of pristine (lower curve) and fully lithiated (upper curve) Li-Fe-O electrodes.

A comparison of the two patterns shows that only a small fraction of the material is left in the original crystalline form. In addition, several new peaks are seen in the pattern of the lithiated Li-Fe-O compound. The new peaks are very broad thus indicating the formation of nano-crystalline phases. The peak assignment process is not completed yet, but two peaks (#12 and #20) certainly belong to metallic iron while peak #7 belongs to Li_2O. Iron and lithium oxide are most likely the products of the irreversible process that takes place in the first cycle in the voltage range between 1 V (vs. Li) and 0.8 V (vs. Li).

To reduce the extent of the initial irreversible lithiation, the pristine Li-Fe-O compound was preliminary reduced ex-situ by addition of lithium hydride (see Experimental). Figure 4 shows the quasi-equilibrium voltage of several rLi-Fe-O compounds as a function of electrochemical inserted lithium content. For comparison the behavior of the pristine material is also reported.

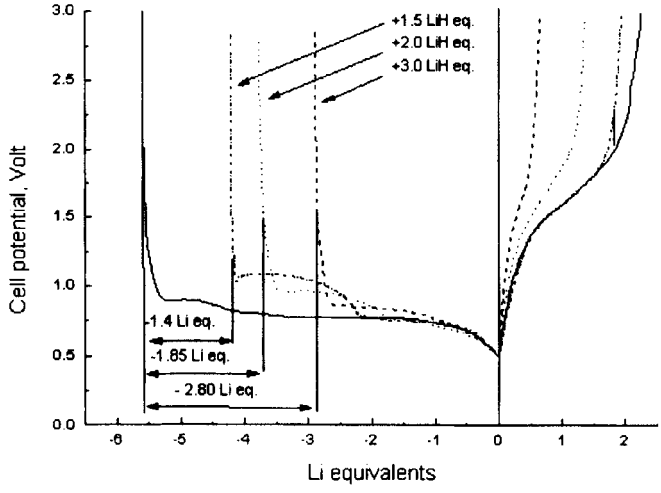

FIGURE 4 Voltage vs. composition behavior of pristine and ex-situ reduced Li-Fe-O electrodes.

The curves were obtained by driving the process in galvanostatic condition at low current density. The extent of the ex-situ reduction, i.e., the equivalents of LiH used, and the Li equivalents corresponding to the decrease of the irreversible capacity, are indicated in the figure. For comparison the quasi-equilibrium voltage behavior of pristine Li-Fe-O compound is also reported. To improve the clarity of the comparison, the curves have been plotted with the end point of the lithium insertion process in the same position. The curves in Figure 4 show the decrease of the lithium inserted (reversibly and irreversibly) in ex-situ reduced compounds during the first discharge (lower numbers). Of further importance, the decrease well matches the extent of the ex-situ chemical reduction process thus confirming the validity of the proposed method. In the following anodic step the compounds release different amounts

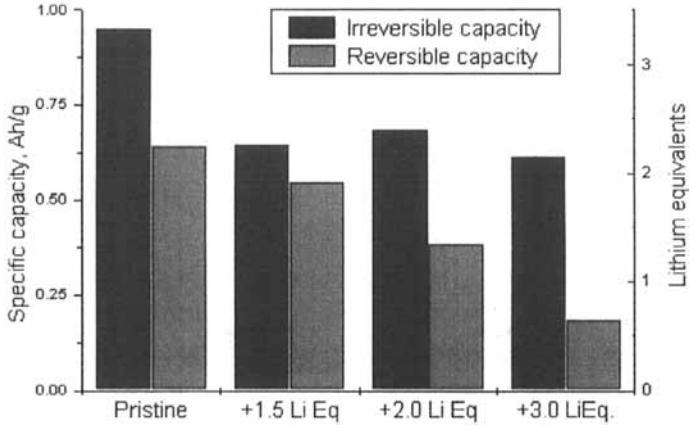

FIGURE 5 First cycle reversible and irreversible capacities of pristine and ex-situ reduced Li-Fe-O materials. The amount of lithium used in ex-situ reduction is indicated in the figure.

of lithium again correlated with the extent of the chemical reduction. However, the ratio of the released/inserted lithium is different for each compound. As shown in Figure 5, the ratio is maximized for the compound preliminary reduced with 1.5 equivalents of LiH per mole of Fe. Of further importance, Figure 5 indicates that: (*i*) the irreversible capacity of all rLi-Fe-O compounds is similar and is lower than in the pristine material; (*ii*) the capacity delivered in the anodic cycle by the rLi-Fe-O (LiH/Fe=1.5) is as large as the one of the pristine material; and (*iii*) the compounds ex-situ reduced with larger amounts of LiH (LiH/Fe>1.5) showed a lower reversible capacity.

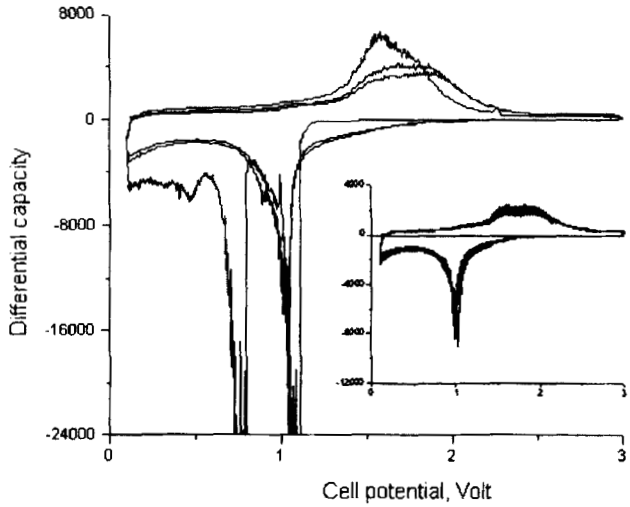

FIGURE 6 Differential capacity vs. electrode voltage behavior of an ex-situ reduced Li-Fe-O (LiH/Fe=1.5) electrode. The figure refers to the first three cycles while the inset illustrates the behavior in following cycles.

The behavior of the reversible and the irreversible capacity with the extent of the ex-situ reduction indicates that two different irreversible processes, separated by a reversible lithium insertion/release step, take place

upon lithium insertion in the Li-Fe-O material. The first irreversible process is certainly related with the first voltage plateau seen in Figure 1 and with the first cathodic peak in the differential capacity vs. voltage plot of Figure 2. This process takes place electrochemically in the pristine Li-Fe-O material or chemically in the ex-situ reduced compounds. As a matter of the fact, all rLi-Fe-O compounds show a similar reduction in the irreversible capacity. It involves the irreversible reduction of the Li-Fe-O material with 1.0 equivalents of lithium (1.0 mole of electrons). At lower voltage the reversible lithium

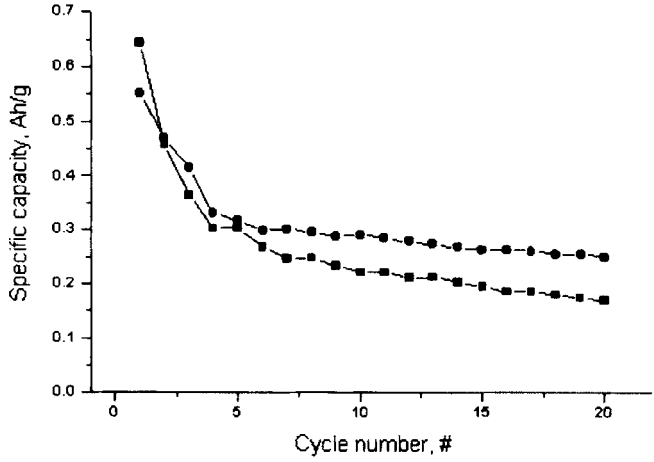

FIGURE 7 Comparison of pristine (square) and ex-situ reduced Li-Fe-O (circle) (LiH/Fe=1.5) electrodes upon cycling.

insertion process takes place. The corresponding voltage plateau is well seen in the quasi-equilibrium voltage vs. composition curve of rLi-Fe-O (LiH/Fe=1.5) in Figure 4. The reversibility of this process is confirmed by the reversible capacity decrease of the more extensively ex-situ reduced materials (Figure 5). Surprisingly the plateau is shifted at a higher voltage than in the pristine

material. Finally, a second irreversible process takes places. The extent of this process is about 2 Li equivalents.

Figure 6 shows the differential capacity behavior of the rLi-Fe-O (LiH/Fe=1.5) material. The two peaks associated to the reversible process and the irreversible (second) process are well seen. As noted earlier, the reversible process is shifted toward higher voltages (1.1 Volt vs. Li) than in pristine Li-Fe-O. The reversible peak does not shift substantially on cycling as shown in the inset. The peak seen at lower voltages is certainly associated with the irreversible process as indicated by its disappearance in following cycles.

Figure 7 illustrates the cycling behavior of the rLi-Fe-O (LiH/Fe=1.5) compound. For comparison, the cycling behavior of the pristine Li-Fe-O material is also reported. The figure clearly shows the improved performance of the latter compound. Although the pristine material shows a larger initial capacity it is affected by a larger capacity fading. At the second cycle the two materials delivered about the same capacity. From this point onwards the lower capacity fading showed by the ex-situ reduced compound led it to deliver larger capacities (ca. 275 mAh/g) than the pristine Li-Fe-O material.

CONCLUSION

A non-stoichiometric Li-Fe-O compound was synthesized by solid-state reaction of Li_2CO_3 and Fe_2O_3 at high temperature. The material was tested as intercalation negative electrode for lithium batteries. A large irreversible capacity affects the electrode during the first discharge cycle. The fraction of the charge irreversible lose exceeds the fraction that can be reversible recovered of about 1.5 times. However the material offered a specific capacity of about 640 mAh/g at the first cycle. The specific capacity continuously decreases upon cycling confirming that the lithium insertion process is not completely reversible.

It was demonstrated that performing an ex-situ reduction with lithium

hydride prior use in battery can reduce the initial irreversible capacity of the material.

The reaction with lithium hydride both affects the charge and discharge capacities. The ratio of these quantities depends of the extent of the ex-situ reduction process and it is maximized for the compound reduced using 1.5 equivalents of LiH per mole of Fe. Although the pristine material shows a larger initial capacity, a lower capacity fading led the reduced material to deliver larger capacities than the pristine Li-Fe-O material upon cycling.

The procedure used is general and can be applied to other metal oxides to use as alternative negative electrodes for lithium ion batteries.

Acknowledgments

The authors would like to thank **MICA** (**M**inistero per l'**I**ndustria, il **C**ommercio e l'**A**rtigianato) for the financial support. Dr. S. Loreti (ENEA) is kindly acknowledged for helpful discussion.

References

[1] T. Shodai, S. Okada, S. Tobishima and J. Yamaki, Solid State Ionics, **86,** 785 (1996).
[2] S. Suzuki and T. Shodai Solid State Ionics, **116,** 1 (1999).
[3] J.J. Auborn and Y.L. Barbero, J. Electrochem. Soc., **134,** 638 (1987).
[4] Watanabe, Atsushi, Kato and Toshiyuki, Jpn. Pat. Appl., 91/119,321, 23 April 1991.
[5] E. Ferg, J. Gummow, A. de Kock and M.M. Thackeray, J. Electrochem. Soc., **141,** L147 (1994).
[6] T. Ohzuku, A. Ueda and N. Yamamoto, J. Electrochem. Soc., **142,** 1431 (1995).
[7] S.Y. Huang, L. Kavan, I. Exnar and M. Gratzel, J. Electrochem. Soc., **142,** L142 (1995).
[8] M.A. Cochez, J.C. Jumax, P. Lavela, J. Morales, J. Olivier-Fourcade and J.L. Tirado, J. Power Sources, **62,** 101 (1996).
[9] Y. Idota, M. Mishima, Y. Miyaky and T. Miyasaka, U.S. Patent 5, 618, 640 (1997).
[10] Y. Idota, T. Kubota, A. Matsufuji, Y. Maekawa and T. Miyasaka, Science, **276,** 1359 (1997).
[11] I.A. Courtney and J.R. Dahn, J. Electrochem. Soc., **144,** 2045 (1997).
[12] B.A. Boukamp, G.C. Lesh and R.A. Huggins, J. Electrochem. Soc., **128,** 725 (1981).
[13] J. Wang, I.D. Raistrick and R.A. Huggins, J. Electrochem. Soc., **133,** 457 (1986).
[14] T. Ohzuku, Z. Thakehara and S. Yoshizawa, Denki Kagaku, **46,** 411 (1978).
[15] B. Di Pietro, M. Patriarca and B. Scrosati, J. Power Sources, **8,** 289 (1982).
[16] K.M. Abraham, D.M. Pasquariello and E.B. Willstaedt, J. Electrochem. Soc., **137,** 743 (1990).
[17] S. Hua, G. Cao and Y. Cui, J. Power Sources, **76,** 112 (1998).